Molecular Conformation and Intermolecular Interactions of Linear and Cyclic Amylose Derivatives in Solution

Ken Terao, Akiyuki Ryoki, Shinichi Kitamura, and Takahiro Sato*

K. Terao, A. Ryoki, T. Sato
Department of Macromolecular Science, Graduate School of Science, Osaka University, 1-1 Machikaneyama-cho, Toyonaka, Osaka 560-0043, Japan
E-mail: terao.ken.sci@osaka-u.ac.jp

A. Ryoki
Department of Polymer Chemistry, Graduate School of Engineering, Kyoto University, Katsura, Kyoto 615-8510, Japan

S. Kitamura
Center for Research and Development of Bioresources, Organization for Research Promotion, Osaka Prefecture University, 1-2, Gakuen-cho, Naka-ku, Sakai, 599-8570, Japan

Keywords: ring polymers; polysaccharide derivatives; helical structure; chain stiffness; chiral separation; liquid crystallinity

Abstract:

Four kinds of rigid and semiflexible ring polymers were synthesized from flexible cyclic amylose. Their conformational properties in dilute solution were determined from dimensional and hydrodynamic properties in terms of the wormlike ring model. The helix rise per residue h of some ring polymers is larger or smaller than that for the corresponding linear chains, indicating that the local helical structure of the ring polymer is not the same as that for the linear chain. Intermolecular interactions detected by the second virial coefficient and chiral recognition ability of some ring polymers are different from the linear chain, suggesting the local structural change causes the intermolecular interactions. We also found that rigid ring polymers can form liquid crystal phase at high concentration. X-ray diffraction results suggest that the ring chains form pseudo rodlike conformation in the liquid crystal phase, showing that intermolecular excluded volume effects significantly influence the conformation of the polymer chains.

1. Introduction

Rigid ring polymers for which local curvature can be different from that for the linear chain while those for the flexible chains are substantially the same as each other. Thus, the polymer segments of rigid ring polymers are somewhat different from those for the linear chain as illustrated in Figure 1. Indeed, tubular self-assembly was revealed by the macrocyclic brush copolymers,[1] and specific smectic phases are theoretically predicted for rigid nanorings.[2] The conformational difference from the linear chain can also influence not only the local conformation but also the intermolecular interactions. Rigid ring polymers are thus promising candidate materials for the building block of nanostructures. However, few works have been done for the rigid ring polymers because of the difficulty to realize such polymers except for double helical cyclic DNA[3] and grafted ring polymers.[1, 4, 5] The electrostatic repulsion of DNA and long side groups of the graft polymers however complicate the discussion on the detailed conformation and intermolecular interactions of rigid ring polymers. Enzymatically synthesized cyclic amylose[6] may be a good starting material of the rigid ring because cyclic amylose behaves as relatively flexible ring chains in solution[7, 8] and three hydroxy groups of each repeat unit can be readily modified without main chain scission. We thus firstly synthesized cyclic amylose tris(phenylcarbamate)[9] (cATPC) which behaves as typical semirigid ring in solution. In this paper, we abstract our recent results for the cyclic amylose derivatives in solution, that is, the molecular conformation in dilute solution, intermolecular interactions including chiral recognition ability, and lyotropic liquid crystallinity in the concentrated solution, after we briefly explain the chain conformation of linear amylose derivatives in solution.

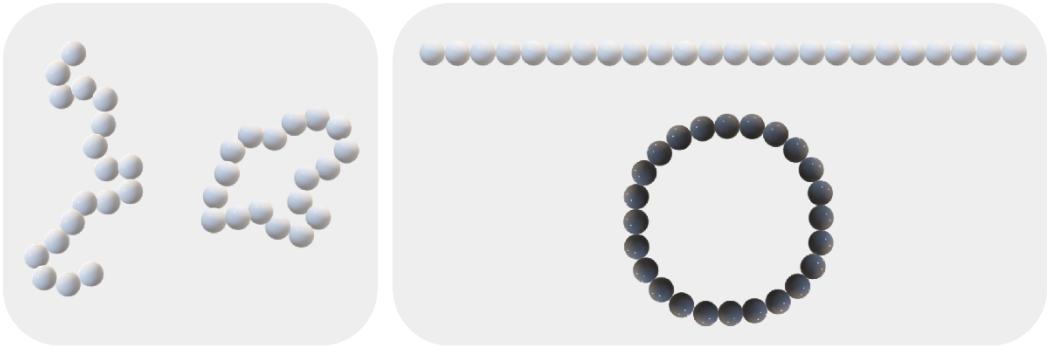

Figure 1. Schematic representation of the segments (or local curvature) of linear and ring polymers. (a) Flexible chains, (b) Rigid (stiff) chains.

2. Chain Conformation of Linear Amylose Carbamates

It is well-known that amylose tris(phenylcarbamate) (ATPC) has higher chain stiffness than the cellulose analog in solution since 1960's.[10, 11] However, the specific helical nature of amylosic chains made difficult to evaluate accurately the chain stiffness parameter, the Kuhn segment length L_K, in terms of the Kratky-Porod wormlike chain,[12, 13] because the local helical structure of amylosic chains may influence the contour length L of the polymer, or helix rise per residue h defined as $L = Nh$ with N being the degree of polymerization. Recent development of synchrotron-radiation small-angle X-ray scattering (SR-SAXS) equipment allows us to determine unequivocally the two parameters, h and L_K. We thus determined both parameters accurately from SR-SAXS, static and dynamic light scattering, and viscometry by means of the latest theories[13] for the wormlike chain with or without the intramolecular excluded-volume effect to find both the parameters are significantly influenced by the side group and solvents. We summarize the parameters for ATPC,[14, 15] amylose tris(ethylcarbamate) (ATEC),[16] amylose tris(*n*-butylcarbamate) (ATBC),[17-19] amylose tris(*n*-hexylcarbamate) (ATHC),[16] amylose tris(*n*-octadecylcarbamate) (ATODC),[20] amylose tris(3,5-dimethylphenylcarbamate) (ADMPC),[21] and amylose-2-acetyl-3,6-bis(phenylcarbamate) (AAPC)[22] in Figure 2. The

different plots with the same symbol mean the different solvent systems. Actual parameters are summarized in our recent review[23] except for ATODC.[20] The *h* value related to the average helical structure of the polymer in solution varies from 0.25 nm to 0.42 nm. This is consistent with that amylose[24-27] and amylose esters[28, 29] have different crystal structures with the *h* value from 0.10 nm to 0.40 nm. Indeed, a shallow minimum with various *h* was found in the conformational energy map both for amylose[7, 30] and ADMPC.[31] On the other hand, the chain stiffness L_K distributes in a wider range from 9 nm to 75 nm. The highest value is smaller than double helical xanthan[32] and triple helical schizophyllan[33] but still much larger than that for amylose,[34, 35] cellulose carbamates,[36-38] and hyaluronan.[39, 40] The chain stiffness for amylose carbamates with small side groups, ATEC and ATBC, are mostly determined by the intramolecular hydrogen bonding between NH and C=O groups on the neighboring glucose units.[16, 17, 23] Hydrogen bonding solvent molecules can extend the helical structure and stiffen the main chain for the amylose carbamates with bulky side groups, especially for ADMPC,[21] ATPC,[15] and ATODC.[20] Similar variation of *h* and L_K was also found for cellulose[38] and curdlan[41] derivatives while they are less significant than those for amylose. Furthermore, since ATPC[15] and ATBC[18] have LCST and UCST type theta temperatures, respectively, at which the second virial coefficient vanishes, amylose carbamate derivatives are suitable to investigate intermolecular interactions of the corresponding ring polymers as described below.

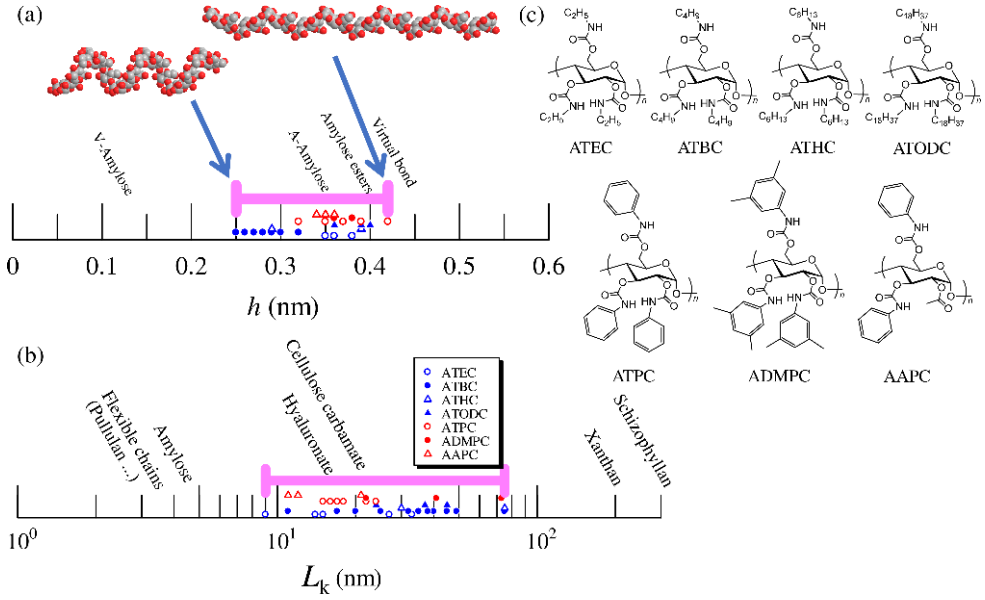

Figure 2. Wormlike chain parameters in linear amylose derivatives in solution.[14-22] (a) Helix rise per residue h. (b) The Kuhn segment length L_k. (c) Chemical structure of the amylose derivatives investigated.

3. Preparation of Ring Amylose Derivatives and the Conformational Properties in Solution

Four ring amylose derivatives with different side groups as illustrated in Figure 3 were synthesized from cyclic amylose which was prepared in the manner reported previously.[6, 8] The linear contaminant may be negligibly few amounts because cADMPC is soluble in THF despite low solubility of ADMPC in the solvent at room temperature. The weight-average degree of polymerization N_w ranges between 30 and 200. The ring shape can be confirmed by the AFM image of a cADMPC sample as shown in Figure 4.[42] The L_K value of the corresponding linear chain in the investigated solvents listed below varies from 11 nm to 75 nm. The Kuhn segment number (L / L_K) thus ranges from 0.1 to 7, covering rigid and semiflexible ring chains.

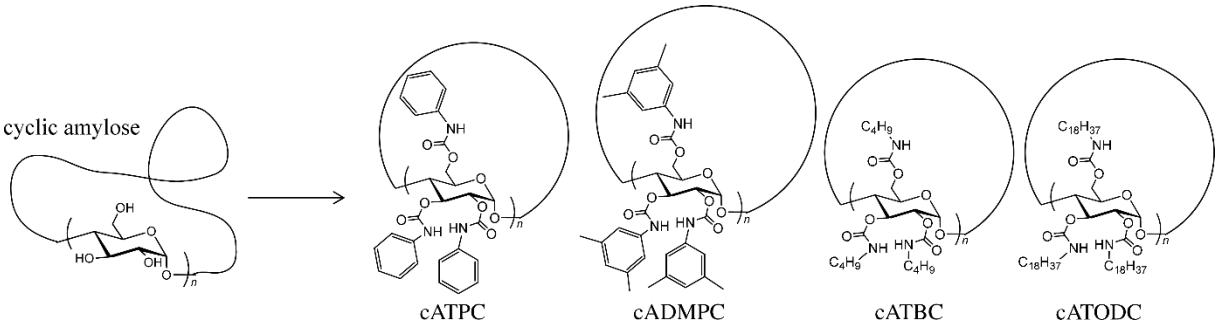

Figure 3. Chemical structures of cyclic amylose, cyclic amylose tris(phenylcarbamate) (cATPC), cyclic amylose tris(3,5-dimethylphenylcarbamate) (cADMPC), cyclic amylose tris(*n*-butylcarbamate) (cATBC), and cyclic amylose tris(*n*-octadecylcarbamate) (cATODC).

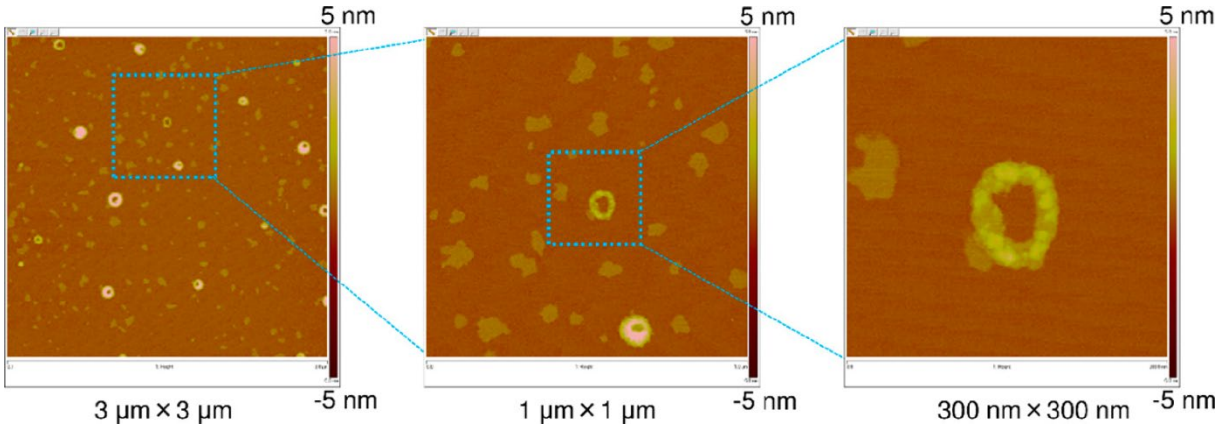

Figure 4. AFM images for a cADMPC sample on a mica surface. Reprinted with permission from ref. [42]. Copyright 2017, American Chemical Society.

Chain conformation in dilute solution was examined for cATPC in 1,4-dioxane (DIOX), 2-ethoxyethanol (2EE), methyl acetate (MEA), ethyl acetate (EA), and 4-methyl-2-pentanone (MIBK), cADMPC in tetrahydrofuran (THF), MEA, and MIBK, cATBC in THF, methanol, 2-propanol (2PrOH), and L-ethyl lactate (EL), and cATODC in THF, *tert*-butyl methyl ether (MTBE), and 2-octanone (MHK) by means of SR-SAXS and dynamic light scattering (DLS) to determine the form factor $P(q)$, the radius of gyration R_g, and the hydrodynamic radius R_H. The obtained dimensional and hydrodynamic properties were analyzed in terms of the modern theories for the wormlike ring.[43-45] Consequently, we found that both the h and L_K values for the ring chains can be different from those for the linear chains. We thus determined the two

parameters from $P(q)$ for each sample because the parameters for ring polymers can depend on the molar mass. The evaluated h ratio of ring to linear (h_{ring} / h_{linear}) are plotted against the Kuhn segment number $(L / L_K)_{linear}$ for the corresponding linear chain in Figure 5(a). It should be noted that the error range of h_{ring} is mostly between 5 and 10% and that of $L_{K,ring}$ is between 10 and 35% for which the actual ranges are shown in the original papers.[20, 42, 46] Most data without cATPC in MEA, EA, and MIBK are plotted because they have specific phenomena described below. While the h_{ring} / h_{linear} data in the range of $(L / L_K)_{linear} > 1$ are dispersed around unity, almost all h_{ring} / h_{linear} values are larger than unity for the smaller $(L / L_K)_{linear}$ range, suggesting that local helical structure of the rigid ring polymers are somewhat extended. The difference between linear and ring chains are more significant for the chain stiffness as is shown in Figure 5(b) in which the chain stiffness ratio $L_{K,ring}$ / $L_{K,linear}$ are plotted against $(L / L_K)_{linear}$. Interestingly, the difference becomes appreciable below $(L / L_K)_{linear} = 1$ where ring closure probability for the (linear) wormlike chain rapidly decreases with shortening chain length (or stiffening the main chain).[47] Consequently, we conclude that the topological constraint of rigid ring polymers may influence the local helical conformation of the amylose main chain.

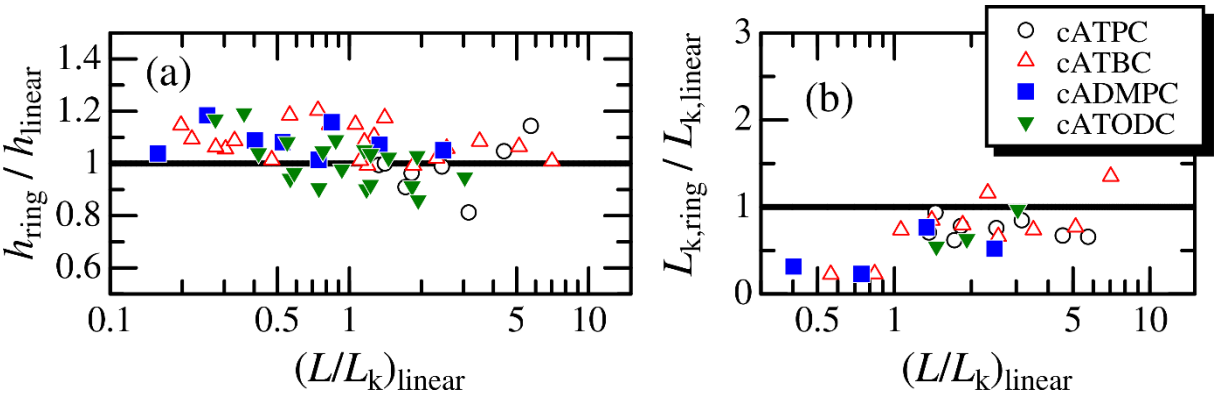

Figure 5. Comparison of the wormlike chain parameters between ring and linear amylose derivatives. Unfilled circles, cATPC in 1,4-dioxane (DIOX) and 2-ethoxyethanol (2EE).[46] Unfilled triangles, cATBC.[46, 48] Filled squares, cADMPC,[42] filled inverse triangles, cATODC.[20] (a) The ratio of the h values for ring and linear plotted against the reduced chain

length $(L/L_k)_{linear}$ for the corresponding linear chain. (b) The ratio of the L_K values for ring and linear are plotted against $(L/L_k)_{linear}$. Reprinted with permission of ref. [48]. Copyright 2021, American Chemical Society.

4. Specific Polymer-Solvent Interactions of cATPC in Ketones and Esters

The above-mentioned local conformational difference between linear and ring polymers can influence the polymer-solvent interactions. In this section, we introduce cATPC in ketones and esters because the detectable difference in the polymer-solvent interactions was observed. According to Fujii et al.,[15] the intrinsic viscosity of ATPC in ketones and esters tends to increase with increasing molar volume v_M of the solvent. Analyses of the dimensional and hydrodynamic properties showed that both the h and L_K values increase with v_M in the solvents, suggesting hydrogen-bonding solvent molecules to the NH group of ATPC extend the local helical structure and stiffen the main chain of the polymer. Figure 6(a) displays the h_{ring} / h_{linear} values for cATPC in MEA, EA, and MIBK (filled circles) along with those in DIOX and 2EE (unfilled circles). Ryoki et al.[46] found that the h_{ring} / h_{linear} values in the ketones and esters are appreciably smaller than unity while those in the ethers (DIOX and 2EE) are substantially close to 1. The small h_{ring} / h_{linear} values for cATPC in the former solvent systems suggest fewer hydrogen bonding solvent molecules for cATPC than those for the linear ATPC in the corresponding solvent.

This specific polymer-solvent interactions can influence the second virial coefficient A_2 which is a measure of the intermolecular interactions between two polymer chains. As is well known that ring polymers show positive A_2 even in the theta solvent[49, 50] because two discreate ring polymers cannot interpenetrate each other. Indeed, the A_2 value for cATBC in 2PrOH is positive (Figure 6b)[51] and can be explained by the simulation data for the wormlike ring.[52] The colored data points in Figure 6(b) indicate the reduced second virial coefficient $(A_2M_L^2/4N_AL_k)$ for cATPC in MEA, EA, and MIBK at the theta temperature where M_L and N_A

denote the molar mass per unit contour length and the Avogadro number, respectively. All the data points are lower than the simulation value and decrease with increasing ν_M. The substantially zero and negative A_2 values in EA and MIBK, respectively, clearly shows the segment-segment interactions of cATPC is more attractive than that for the linear chain. This strongly supports the above-suggested fewer solvation of cATPC than that of ATPC. In other words, interpolymer and/or polymer-solvent interactions can be influenced by the topology of the semiflexible and rigid ring polymers.

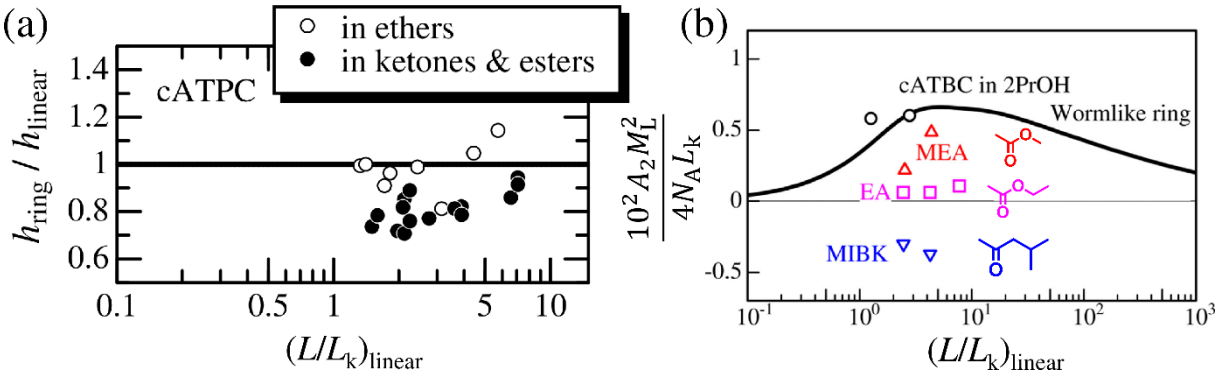

Figure 6. (a) The ratio of h values for ring and linear polymers plotted against $(L/L_k)_{linear}$ for cATPC in ethers (unfilled circles) and in ketones and esters (filled circles). (b) Reduced chain length $(L/L_k)_{linear}$ dependence of the reduced second virial coefficient $(A_2M_L^2/4N_AL_k)$ for cATPC in MEA (unfilled triangles), EA (unfilled squares), and MIBK (inverted triangles) at the corresponding theta temperatures along with the data for cATBC in 2PrOH.[51] Solid curve is the data from Monte Carlo simulation by Ida et al.[52] Reprinted with permission from ref. [53]. Copyright 2013, American Chemical Society.

5. Different Chiral Separation Ability of Ring Polymer

One of the prominent functions of polysaccharide carbamate derivatives is the use of the chiral separation column for the HPLC system.[54-56] Okamoto et al. showed both ATPC[57] and ADMPC[58] have high chiral separation ability and the latter is commercially available as

the chiral stationary phase (CSP) for the HPLC column. Taking into consideration that the intermolecular interactions between side groups of ADMPC and chiral molecules are one of the key factors of the chiral separation, local structural difference between cADMPC and ADMPC may cause the difference in the chiral separation ability. We thus coated cADMPC or ADMPC on wide pore silica gel to prepare CSPs.[59] The resulting columns were tested with 8 racemates to compare their chiral separation ability. Figure 7 shows some representative chromatograms for flavanone and benzoin with the eluent of *n*-hexane/2-propanol (9/1). As is clearly seen that flavanone can be separated only by the cADMPC column while benzoin has an opposite behavior. This clearly shows that the chain conformation on the silica gel is definitely important for the chiral separation ability. In other words, not only chemical structures of main and side chains but also the local conformation of the polymer chains play an important role for high-performance polysaccharide based CSPs.

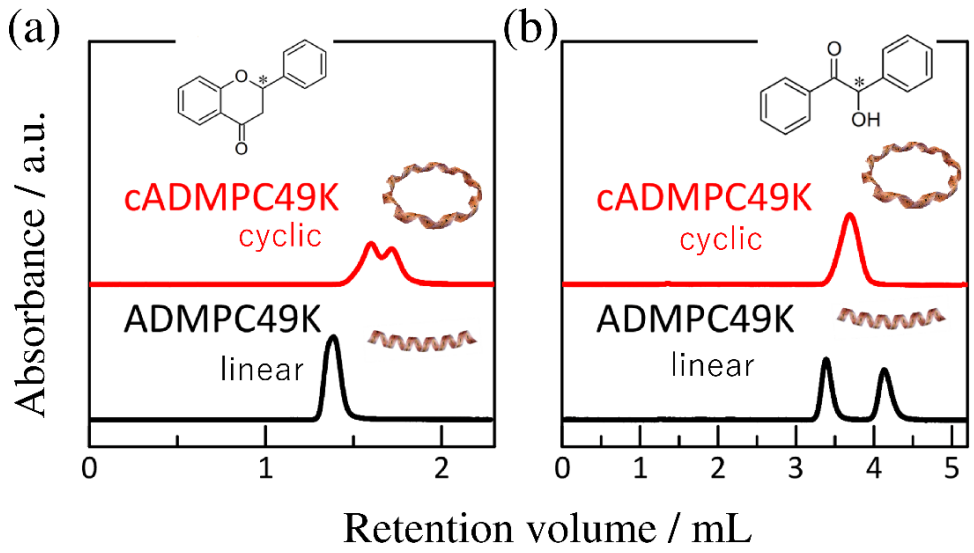

Figure 7. (a) Chromatograms of (a) flavanone and (b) benzoin on indicated CSPs using *n*-hexane/2-propanol (9/1) as the eluent. Reprinted with permission from ref. [59]. Copyright 2019, Elsevier.

6. Lyotropic Liquid Crystallinity and Chain Alignment of Rigid Ring Polymers.

Concentrated solutions of rigid polymers may have significant birefringence, that is, lyotropic liquid crystallinity. Many semiflexible and rigid linear polymers form the nematic phase in which the polymer chains align parallel.[60] There is, however, few studies for rigid nonlinear polymers except for three arm star polymers with rigid arm chains[61, 62] and superhelical cyclic DNA.[63] Recently, we estimated the star chains can form pseudo rodlike conformation from the X-ray diffraction and the phase diagram[62] because the crosslinking point of three arms are relatively flexible.[64] On the other hand, Avendano et al.[2] predicted theoretically that the rigid nanorings can form smectic mesophase at low concentration. We thus determined isotropic-liquid crystal phase boundaries and X-ray diffraction pattern of the concentrated solutions of cATBC[48] in THF and EL and cATODC[65] in THF and MHK. Figure 8 shows the M_w dependence of the phase boundary concentrations c_I and c_A for cATBC and cATODC in THF along with those for the linear chains,[66] where c_I is the phase boundary concentration between isotropic and biphasic regions and c_A is that between biphasic and anisotropic regions. The obtained c_I and c_A for cATBC are almost the same as that for linear ATBC while those for cATODC are somewhat higher than those for the linear chains. Similar behavior was also found for the other solvent systems. This is inconsistent with the above-mentioned theoretical prediction when the ring chains keep the rigid ring conformation in the concentrated solution.

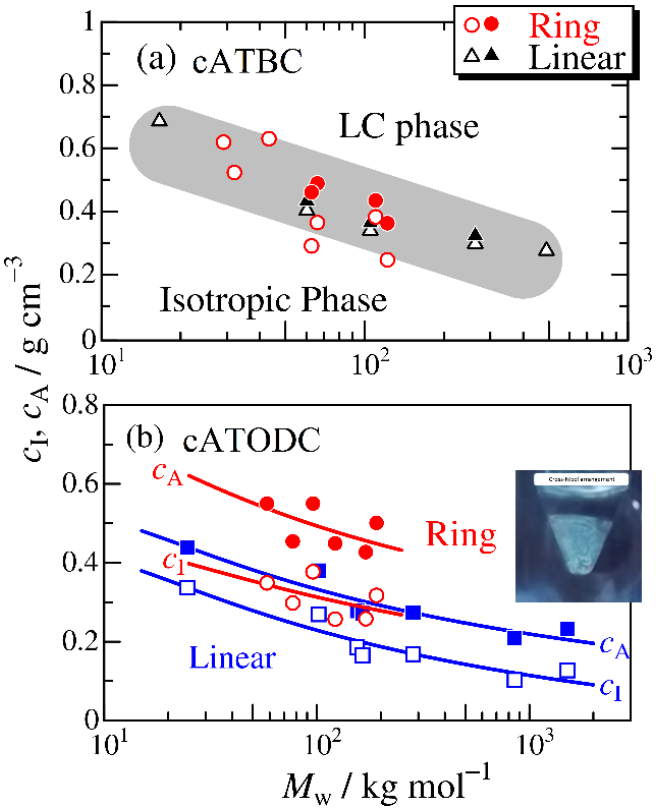

Figure 8. Weight-average molar mass M_w dependence of the phase boundary concentrations, c_I (unfilled circles) and c_A (filled circles) for (a) cATBC and (b) cATODC in THF at 25 °C along with those for linear polymer (triangles and squares). Reprinted with permission from refs. [65] and [48]. Copyright 2019 and 2021, American Chemical Society.

Figure 9 illustrates the X-ray diffraction pattern for the concentrated THF solution of the cATBC and ATBC. The concentrations were higher than c_A. While the scattering profile for **ATBC148K** shows four broad peaks in the q range from 0.06 and 0.2 nm^{-1}, no peaks were found for cATBC samples in the low q range, avoiding smectic structure. It should be noted that the peaks for linear ATBC corresponds to the cholesteric structure. On the contrary, all the solutions including linear and ring polymers have similar sharp peaks in the higher q region from 3 and 10 nm^{-1}. According to our recent paper,[48] these peaks can be assigned as hexagonally (unfilled circles) and tetragonally (filled squares) packed cylinders. If we consider that the linear ATBC aligns parallel in the concentrated solutions, the current diffraction results

indicate the ring polymers should have pseudo rodlike conformation in the high concentrated solutions. This is most likely due to higher intermolecular excluded volume effects of rigid rings than rods. The phase boundary concentrations in Figure 8 can be explained by the scaled particle theory for linear semirigid cylinders with the length (L_{SC} in Figure 9) being half of the contour length and the diameter d_{SC},[48] supporting the pseudo rod conformation.

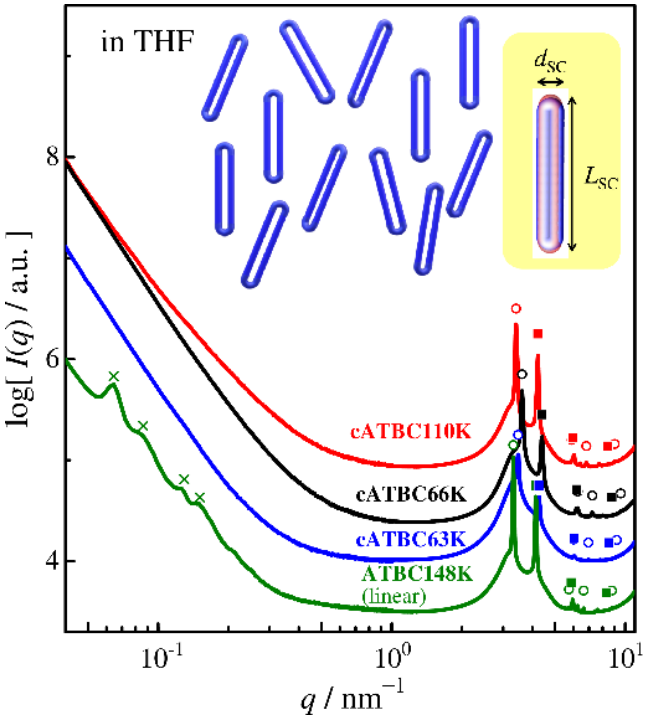

Figure 9. Plots of scattering intensity $I(q)$ versus q for **cATBC110K** (red, c = 0.484 g cm^{-3}), **cATBC66K** (black, c = 0.475 g cm^{-3}) , **cATBC63K** (blue, c = 0.476 g cm^{-3}), and **ATBC148K** (green, c = 0.494 g cm^{-3}) all in THF at 25 °C. Reprinted with permission from [48]. Copyright 2021, American Chemical Society.

7. Conclusion

Rigid and semiflexible ring polymers can be successfully prepared from cyclic amylose with a one-pot reaction. The obtained polymer has appreciably different local conformation comparing with the corresponding linear chain. This is a characteristic feature of the rigid ring

polymer which cannot be seen for the flexible ring polymers. This conformational difference between ring and linear chains can cause the significant change in the interpolymer interactions, polymer-solvent interactions, and polymer-small molecules interactions, which is recognizable by the appreciable difference in the chiral separation ability of the chiral stationary phases made of linear and ring polymers. Investigation of the specific molecular recognition ability of the cyclic chains will be extended to the aqueous systems since both amphiphilic[67] and thermo-responsive[68] amylose derivatives have been obtained. Intermolecular interactions of concentrated ring polymer solutions change the conformation of the ring polymers itself by means of the intermolecular excluded volume effect. This concentration-dependent conformational change of the ring polymer can be affected to the other physical properties including the chain dynamics.

Acknowledgements

This work was partly supported by JSPS KAKENHI grant numbers JP20H02788, JP18J10648, JP17K05884, JP25410130, and JP23750128. The synchrotron radiation experiments were performed at the BL40B2 in SPring-8 with the approval of the Japan Synchrotron Radiation Research Institute (JASRI) (proposal nos. 2010B1126, 2011A1049, 2011B1068, 2013A1046, 2014B1087, 2015A1179, 2015B1100, 2016A1053, 2016B1088, 2018A1124, 2018B1088, 2019A1072, and 2019B1113) and at the BL-10C and BL-6A beamline in KEK-PF under the approval of the Photon Factory Program Advisory Committee (proposal nos. 2010G080, 2011G557, 2013G516, 2015G543, and 2018G516).

Received: ((will be filled in by the editorial staff))

Revised: ((will be filled in by the editorial staff))

Published online: ((will be filled in by the editorial staff))

References

[1] M. Schappacher, A. Deffieux, *Science* **2008**, *319*, 1512.
[2] C. Avendano, G. Jackson, E. A. Muller, F. A. Escobedo, *Proc. Natl. Acad. Sci. U. S. A.* **2016**, *113*, 9699.
[3] A. D. Bates, A. Maxwell, "*DNA topology"*, Oxford University Press, USA, 2005.
[4] S. H. Lahasky, W. K. Serem, L. Guo, J. C. Garno, D. H. Zhang, *Macromolecules* **2011**, *44*, 9063.
[5] K. Zhang, G. N. Tew, *React. Funct. Polym.* **2014**, *80*, 40.
[6] T. Takaha, M. Yanase, H. Takata, S. Okada, S. M. Smith, *J. Biol. Chem.* **1996**, *271*, 2902.
[7] J. Shimada, H. Kaneko, T. Takada, S. Kitamura, K. Kajiwara, *J. Phys. Chem. B* **2000**, *104*, 2136.
[8] Y. Nakata, K. Amitani, T. Norisuye, S. Kitamura, *Biopolymers* **2003**, *69*, 508.
[9] K. Terao, N. Asano, S. Kitamura, T. Sato, *ACS Macro Lett.* **2012**, *1*, 1291.
[10] W. Burchard, *Br. Polym. J.* **1971**, *3*, 214.
[11] W. Burchard, "Light Scattering from Polysaccharides as Soft Materials", in *Soft Matter Characterization*, R. Borsali and R. Pecora, Eds., Springer Netherlands, 2008, p. 463.
[12] O. Kratky, G. Porod, *Recl. Trav. Chim. Pays-Bas* **1949**, *68*, 1106.
[13] H. Yamakawa, T. Yoshizaki, "*Helical Wormlike Chains in Polymer Solutions, 2nd ed."*, Springer, Berlin, Germany, 2016.
[14] K. Terao, T. Fujii, M. Tsuda, S. Kitamura, T. Norisuye, *Polym. J.* **2009**, *41*, 201.
[15] T. Fujii, K. Terao, M. Tsuda, S. Kitamura, T. Norisuye, *Biopolymers* **2009**, *91*, 729.
[16] K. Terao, F. Maeda, K. Oyamada, T. Ochiai, S. Kitamura, T. Sato, *J. Phys. Chem. B* **2012**, *116*, 12714.
[17] K. Terao, M. Murashima, Y. Sano, S. Arakawa, S. Kitamura, T. Norisuye, *Macromolecules* **2010**, *43*, 1061.
[18] Y. Sano, K. Terao, S. Arakawa, M. Ohtoh, S. Kitamura, T. Norisuye, *Polymer* **2010**, *51*, 4243.
[19] S. Arakawa, K. Terao, S. Kitamura, T. Sato, *Polym. Chem.* **2012**, *3*, 472.
[20] A. Ryoki, D. Kim, S. Kitamura, K. Terao, *Polymer* **2018**, *137*, 13.
[21] M. Tsuda, K. Terao, Y. Nakamura, Y. Kita, S. Kitamura, T. Sato, *Macromolecules* **2010**, *43*, 5779.
[22] M. Tsuda, K. Terao, S. Kitamura, T. Sato, *Biopolymers* **2012**, *97*, 1010.
[23] K. Terao, T. Sato, "Conformational Properties of Polysaccharide Derivatives", in *Bioinspired Materials Science and Engineering*, G. Yang and L. Lamboni, Eds., 2018, p. 167.
[24] D. Popov, A. Buleon, M. Burghammer, H. Chanzy, N. Montesanti, J. L. Putaux, G. Potocki-Veronese, C. Riekel, *Macromolecules* **2009**, *42*, 1167.
[25] Y. Nishiyama, K. Mazeau, M. Morin, M. B. Cardoso, H. Chanzy, J. L. Putaux, *Macromolecules* **2010**, *43*, 8628.
[26] M. B. Cardoso, J. L. Putaux, Y. Nishiyama, W. Helbert, M. Hytch, N. P. Silveira, H. Chanzy, *Biomacromolecules* **2007**, *8*, 1319.
[27] Y. Takahashi, T. Kumano, S. Nishikawa, *Macromolecules* **2004**, *37*, 6827.
[28] P. Zugenmaier, H. Steinmeier, *Polymer* **1986**, *27*, 1601.
[29] Y. Takahashi, S. Nishikawa, *Macromolecules* **2003**, *36*, 8656.
[30] C. V. Goebel, D. Brant, W. Dimpfl, *Macromolecules* **1970**, *3*, 644.
[31] C. Yamamoto, E. Yashima, Y. Okamoto, *J. Am. Chem. Soc.* **2002**, *124*, 12583.
[32] T. Sato, T. Norisuye, H. Fujita, *Macromolecules* **1984**, *17*, 2696.
[33] Y. Kashiwagi, T. Norisuye, H. Fujita, *Macromolecules* **1981**, *14*, 1220.
[34] Y. Nakanishi, T. Norisuye, A. Teramoto, S. Kitamura, *Macromolecules* **1993**, *26*, 4220.

[35] X. Y. Jiang, S. Kitamura, T. Sato, K. Terao, *Macromolecules* **2017**, *50*, 3980.
[36] F. Kasabo, T. Kanematsu, T. Nakagawa, T. Sato, A. Teramoto, *Macromolecules* **2000**, *33*, 2748.
[37] X. Y. Jiang, T. Sato, K. Terao, *Polym. Bull.* **2018**, *75*, 1265.
[38] X. Y. Jiang, A. Ryoki, K. Terao, *Polymer* **2017**, *112*, 152.
[39] K. Hayashi, K. Tsutsumi, F. Nakajima, T. Norisuye, A. Teramoto, *Macromolecules* **1995**, *28*, 3824.
[40] K. Hayashi, K. Tsutsumi, T. Norisuye, A. Teramoto, *Polym. J.* **1996**, *28*, 922.
[41] T. Ochiai, K. Terao, Y. Nakamura, C. Yoshikawa, T. Sato, *Polymer* **2012**, *53*, 3946.
[42] A. Ryoki, H. Yokobatake, H. Hasegawa, A. Takenaka, D. Ida, S. Kitamura, K. Terao, *Macromolecules* **2017**, *50*, 4001.
[43] J. Shimada, H. Yamakawa, *Biopolymers* **1988**, *27*, 657.
[44] M. Fujii, H. Yamakawa, *Macromolecules* **1975**, *8*, 792.
[45] R. Tsubouchi, D. Ida, T. Yoshizaki, H. Yamakawa, *Macromolecules* **2014**, *47*, 1449.
[46] A. Ryoki, D. Ida, K. Terao, *Polym. J.* **2017**, *49*, 633.
[47] H. Yamakawa, T. Yoshizaki, "*Helical Wormlike Chains in Polymer Solutions"*, Springer, Berlin, Germany, 2016.
[48] D. Kabata, A. Ryoki, S. Kitamura, K. Terao, *Macromolecules* **2021**, *54*, 10723.
[49] S. F. Edwards, *Proc. Phys. Soc., London* **1967**, *91*, 513.
[50] S. F. Edwards, *J. Phys. A: Gen. Phys.* **1968**, *1*, 15.
[51] K. Terao, K. Shigeuchi, K. Oyamada, S. Kitamura, T. Sato, *Macromolecules* **2013**, *46*, 5355.
[52] D. Ida, D. Nakatomi, T. Yoshizaki, *Polym. J.* **2010**, *42*, 735.
[53] N. Asano, S. Kitamura, K. Terao, *J. Phys. Chem. B* **2013**, *117*, 9576.
[54] J. Shen, Y. Okamoto, *Chem. Rev.* **2016**, *116*, 1094.
[55] T. Ikai, Y. Okamoto, *Chem. Rev.* **2009**, *109*, 6077.
[56] Y. Okamoto, E. Yashima, *Angew. Chem. Int. Ed.* **1998**, *37*, 1020.
[57] Y. Okamoto, M. Kawashima, K. Hatada, *J. Am. Chem. Soc.* **1984**, *106*, 5357.
[58] Y. Okamoto, R. Aburatani, T. Fukumoto, K. Hatada, *Chem. Lett.* **1987**, *16*, 1857.
[59] A. Ryoki, Y. Kimura, S. Kitamura, K. Maeda, K. Terao, *J. Chromatogr. A* **2019**, *1599*, 144.
[60] T. Sato, A. Teramoto, *Adv. Polym. Sci.* **1996**, *126*, 85.
[61] S. H. Goodson, B. M. Novak, *Macromolecules* **2001**, *34*, 3849.
[62] H. Hasegawa, K. Terao, T. Sato, Y. Nagata, M. Suginome, *Macromolecules* **2019**, *52*, 3158.
[63] S. S. Zakharova, W. Jesse, C. Backendorf, J. R. van der Maarel, *Biophys. J.* **2002**, *83*, 1119.
[64] H. Hasegawa, Y. Nagata, K. Terao, M. Suginome, *Macromolecules* **2017**, *50*, 7491.
[65] D. Kim, A. Ryoki, D. Kabata, S. Kitamura, K. Terao, *Macromolecules* **2019**, *52*, 7806.
[66] K. Oyamada, K. Terao, M. Suwa, S. Kitamura, T. Sato, *Macromolecules* **2013**, *46*, 4589.
[67] Y. Kameyama, S. Kitamura, T. Sato, K. Terao, *Langmuir* **2019**, *35*, 6719.
[68] S. Kimura, R. Kochi, S. Kitamura, K. Terao, *ACS Appl. Polym. Mater.* **2020**, *2*, 2426.